Mathematically reduced reaction mechanisms applied to adiabatic flat hydrogen/air flames

Mathematically Reduced Reaction Mechanisms Applied to Adiabatic Flat Hydrogen/Air Flames

R. L. G. M. EGGELS and L. P. H. de GOEY*

Eindhoven University of Technology, Faculty of Mechanical Engineering (WOC), PO Box 513, 5600 MB Eindhoven, The Netherlands

Several hydrogen/air reaction systems are reduced mathematically to one-step schemes, using the method introduced by Maas and Pope [1]. The reduction is obtained by assuming fast reaction groups of the reaction system to be in steady state. We developed a method to apply the reduced schemes to adiabatic flat flames. The results are compared with those of detailed chemistry calculations. The accuracy of the results of reduction of the most simple reaction system, (which does not include the species HO_2 and H_2O_2) is quite well. The other reaction systems, however, give appreciable errors in burning velocity. This is mainly caused by large deviations in HO_2 mole fractions between reduced and full scheme calculations, while the reaction rate and the burning velocity are sensitive to variations in the mole fraction of HO_2. Considering the time scales of the reaction system and the time scales of convection and diffusion it is shown that at low temperatures, where the mole fraction of HO_2 reaches its maximum, the basic assumptions applied to reduce the mechanisms are not justified. It is concluded that the hydrogen/air system can only be reduced to an accurate one-step reduced scheme, if reaction schemes without HO_2 and H_2O_2 are used. This reduction technique also indicates, in accordance with conclusions of Peters et al. [3], that a two-step reduced scheme has to be used if more realistic hydrogen/air schemes, including HO_2 and H_2O_2, are considered.

1. INTRODUCTION

Numerical calculations of multidimensional combustion processes, including detailed kinetics, require excessive computing power, mainly caused by the large number of species involved. For better understanding of combustion processes as well as for engineering purposes, reduction of the computing effort is required. To reduce the complexity of the system and, therefore, also the demanded computing effort, it is highly desirable to reduce the number of differential equations, without losing too much accuracy. As a result many combustion researchers work [1–6] on the reduction of chemical reactions schemes, nowadays. Conventional reduction methods [2–4] are based on steady-state and partial-equilibrium assumptions. Knowledge of reaction systems is required to decide which species and reactions may be assumed in steady state or in partial equilibrium. Furthermore, each specific combustion problem needs its own reduced mechanism.

An alternative method to simplify chemical kinetics is CSP (Computational Singular Perturbation), introduced by Lam and Goussis [5–6]. This method is based on the separation of the reaction system into slow and fast reaction groups. The decoupling of fast reaction groups makes it possible to solve the stiff set of differential equations, that describe the complex reaction system, fast and efficiently. Moreover, the information on the fast and slow reaction groups, can be used to find out which set of reactions is in partial equilibrium and which species are in steady state, locally. This can be used to develop convential reduced schemes, as described above. An advantage of the method is this can be done automatically. Therefore, less insight in chemical kinetics is required.

The method of Intrinsic Low-Dimensional Manifolds in Composition Space, presented by Maas and Pope [1] is based on the same basic ideas as CSP. This method also separates the full reaction scheme into reaction groups of large and small time scales automatically. The

*Corresponding author.

COMBUSTION AND FLAME 100: 559–570 (1995)

Published by Elsevier Science Inc.

0010-2180/95/$9.50
SSDI 0010-2180(94)00108-5

reduction of the system is obtained by introducing steady-state approximations for the reaction groups corresponding with the smallest time scales. The main difference of this reduction technique and the CSP method is that the manifold, defined by the steady-state assumptions, is parametrized. Moreover, the steady-state equations are calculated beforehand and the solution is stored, making fast flame calculations possible. The difference with conventional reduced schemes is that the steady-state assumptions are neither partial-equilibrium assumptions for elementary reactions nor steady-state assumptions for intermediate species. Furthermore, the steady-state relations for the mathematically reduced scheme are not fixed throughout the combustion process. The dimension (number of differential equations) of the reduced scheme may be chosen appropriately. Note that it is not possible to determine the most appropriate dimension of the reduced mechanism beforehand. The same problem arises if conventional reduction methods are used. However, examination of the eigenvalues on the manifold and comparing these with the time scales of convection and diffusion gives an estimate whether the reduced scheme will be appropriate.

In this article, we study the use of the mathematical reduction technique in the modeling of adiabatic flat premixed hydrogen/air flames. We will restrict ourselves to one-dimensional reduced schemes. The principle of the mathematical reduction technique is explained briefly in Section 2, where we focus on the basic assumptions of the method. In Section 3 we present the method we use to apply the low-dimensional manifold to flat-flames. The results are compared with those of full scheme calculations in Section 4. It appears that differences with full scheme calculations increase when more complex reaction schemes are used. To investigate the source of the differences, we introduce a time scale analysis of the system (Section 5). This analysis indicates that the approximations applied to reduce the reaction scheme are not justified when more complex reaction schemes are used. Higher-order reduction methods have to be used for these reaction mechanisms.

2. MATHEMATICALLY REDUCED SCHEMES

The method followed to reduce complex reaction schemes is presented here briefly. Basically we follow the approach of Maas and Pope [1], who explained the method in more detail.

Consider the conservation equations of the species, given by

$$\rho\frac{\partial \phi_i}{\partial t} + \rho \boldsymbol{v} \cdot \nabla \phi_i - \nabla \cdot (\rho D_i \nabla \phi_i) = \rho W_i, \quad (1)$$

where ϕ_i denotes the specific mole number, defined by Y_i/M_i, with Y_i the mass fraction and M_i the molar mass of species i. The density of the mixture is given by ρ, $\boldsymbol{v}$ is the flow velocity vector, D_i the diffusion coefficient, and W_i the chemical source term of species i. Additional to the conservation equations for the species we have to solve the conservation equations for mass, momentum and enthalpy.

To study the chemical nature of the reaction system we consider a homogeneous system first:

$$\frac{\partial \phi_i}{\partial t} = W_i. \quad (2)$$

The system is described in the n-dimensional composition space where $\boldsymbol{\phi} = (\phi_1, \ldots, \phi_n)^T$ indicates the composition vector, containing the specific mole numbers ϕ_i of the n species. Because reaction processes obey the conservation equations of elements, displacements in composition space are restricted to a $(n - n_e)$ subspace, where n_e denotes the number of elements. For the reduced scheme movements in composition space are even more restricted. Only evolution on a low-dimensional manifold, defined by steady-state assumptions for the fastest reaction groups, is allowed. The number of steady-state assumptions is $(n - n_e - n_c)$, for a n_c-dimensional reduced scheme. Fast and slow reaction groups can be separated by use of an eigenvector analyses of the source term $\boldsymbol{W} = (W_1, \ldots, W_n)^T$, linearized around a reference composition $\boldsymbol{\phi}^0$:

$$\boldsymbol{W} = \boldsymbol{W}(\boldsymbol{\phi}^0) + \frac{\partial \boldsymbol{W}(\boldsymbol{\phi}^0)}{\partial \boldsymbol{\phi}}(\boldsymbol{\phi} - \boldsymbol{\phi}^0). \quad (3)$$

The absolute values of the real parts of the eigenvalues of the Jacobian matrix $\partial \boldsymbol{W}(\boldsymbol{\phi}^0)/\partial \boldsymbol{\phi}$ are the reciprocal values of the typical time scales of the linearized system. This can be seen by considering an instationary homogeneous system in the basis of eigenvectors of $\partial \boldsymbol{W}(\boldsymbol{\phi}^0)/\partial \boldsymbol{\phi}$. In this basis, the eigenvalues are ordered in descending order of real part: $\mathrm{Re}(\lambda_1) \geq \cdots \geq \mathrm{Re}(\lambda_n)$, where $\mathrm{Re}(\lambda_i)$ denotes the real part of eigenvalue i. Then, we may write:

$$\frac{\partial \boldsymbol{\phi}'}{\partial t} = \boldsymbol{W}'(\boldsymbol{\phi}^0) + \Lambda(\boldsymbol{\phi}' - \boldsymbol{\phi}'^0), \tag{4}$$

where $\Lambda = \mathrm{diag}(\lambda_1, \ldots, \lambda_n)$, with λ_i the eigenvalues of the Jacobian matrix. The accents denote the variables in the basis of eigenvectors. As a result of the diagonalization, the differential equations in Eq. 4 are decoupled and the solutions are exponentials with typical time scales given by

$$\tau_i = 1/|\mathrm{Re}(\lambda_i)|. \tag{5}$$

If the eigenvalues are complex, the real and imaginary parts of the complex eigenvectors are used in a modified basis. We now return to the general system (Eq. 1). As the reduction only affects the chemical part and it is assumed that the convective and diffusive parts have larger time scales than the time scales of the reduced scheme, we conclude that the time scales of Eq. 5 are also the time scales of the full reaction system. The steady-state assumptions for the fastest reaction groups are formulated slightly differently than those used by Maas and Pope [1]. This, however, does not affect the results. We use the left eigenvectors ($\boldsymbol{S}_i^L$, $i = 1, n$) of the Jacobian matrix to formulate the steady-state assumptions. These left eigenvectors are defined by

$$\boldsymbol{S}_i^L \frac{\partial \boldsymbol{W}(\boldsymbol{\phi}^0)}{\partial \boldsymbol{\phi}} = \lambda_i \boldsymbol{S}_i^L. \tag{6}$$

As the eigenvalues are ordered in descending order of real part on the diagonal of matrix Λ, the steady-state assumptions are given by

$$\boldsymbol{S}_i^L \boldsymbol{W} = 0, \qquad i = n_e + n_c + 1, \ldots, n. \tag{7}$$

In this paper we only consider the case of adiabatic flames with unit Lewis numbers $\mathrm{Le}_i = \lambda/c_p \rho D_i = 1$. This approximation is not essential for the method but is introduced for simplicity: it reduces the dimension of the manifold. When this assumption is relaxed the specific element mole numbers and enthalpy as additional degrees of freedom.

As we consider unit Lewis numbers and adiabatic flames, the specific element mole numbers χ_j and the enthalpy h are constant throughout the domain and are fixed by the stoichiometry and the temperature of the unburned mixture. Thus, additional to the steady-state equations we also may formulate n_e conservation equations for the elements. These may be written as

$$(\boldsymbol{\mu}_j, \boldsymbol{\phi}) = \chi_j, \qquad j = 1, 2, \ldots, n_e, \tag{8}$$

where $\boldsymbol{\mu}_j$ denotes the element composition vector for element j ($\mu_{i,j}$ is the number of atoms of element j in species i) and χ_j denotes the constant value of the specific element mole number of element j.

Finally, we have to solve n_c differential equations corresponding to the largest time scales together with the steady-state relations (Eq. 7) and the conservation equations for the elements (Eq. 8), instead of the full complex set of Eqs. 1. The solution procedure is separated in two parts. Firstly, the manifold defined by Eqs. 7 and 8 is parametrized by n_c parameters, the so-called controlling variables. Then Eqs. 7 and 8 are solved for all physically reasonable values of the controlling variables and stored in a file. As controlling variable we may choose any linear combination of specific mole numbers as long as there exists only one point on the manifold for given controlling variables. Secondly, n_c differential equations for the controlling variables are solved during the application of the reduced scheme. Knowing the spatial dependence of the controlling variables the mixture composition is found at every position by using the manifold map. In the remaining part of this section we present the method

used to calculate the manifold, in Section 3 the differential equations for the controlling variables are derived.

In this paper we consider one-dimensional reduced schemes ($n_c = 1$) of several hydrogen/air systems. There are two elements O and H—present in the systems, thus $n_e = 2$. Nitrogen is not considered here, since N_2 is treated as an inert species. As controlling variable, denoted as α the specific mole number of H_2O is used. Using the definition of the manifold (Eq. 7) and the conservation equations for elements (Eq. 8) we have to solve

$$\boldsymbol{g} = \boldsymbol{o}, \tag{9}$$

with

$$\begin{aligned} g_1 &= \phi_{H_2O} - \alpha = 0, \\ g_2 &= (\boldsymbol{\mu}_O, \phi) - \chi_O = 0, \\ g_3 &= (\boldsymbol{\mu}_H, \phi) - \chi_H = 0, \\ g_i &= S_i^L \boldsymbol{W} = 0, \qquad i = 4, \ldots, n. \end{aligned} \tag{10}$$

The temperature of a point on the manifold follows from the enthalpy equation:

$$h = \sum_{i=1}^{n} M_i \phi_i \left(h_i^0 + \int_{T_0}^{T} c_{p_i}(\tau)\, d\tau \right) = h_{\text{ref}}, \tag{11}$$

which is fixed for unit Lewis numbers. Here, h_i^0 denotes the heat of formation per unit mass, at some reference temperature T_0, c_{p_i}, the specific heat of species i per unit mass at constant pressure and h_{ref} the constant value of the enthalpy, given by the condition of the unburned mixture.

Newton's method is applied to solve Eq. 9. For initial compositions ϕ^0 outside the convergence area of Newton's method, Eq. 9 is solved by using a time-stepping method, which increases the convergence area of the method. Then, the steady-state equations of Eq. 10 are replaced by

$$g_i = S_i^L \left(\boldsymbol{W} - \frac{\boldsymbol{\phi} - \boldsymbol{\phi}^0}{\Delta t} \right) = 0 \qquad \text{for } i = 4, \ldots, n, \tag{12}$$

where Δt denotes a (small) time step. The other equations of Eq. 10 are not modified. This set of equations is also solved with Newton's method for every time step. The equation set 10 or 12 together with Eq. 11 is solved for all physically reasonable values of the controlling variable. As we use ϕ_{H_2O} as controlling variable, the initial composition is given by $\phi_{H_2O} = 0$ and manifold compositions are calculated for increasing H_2O-specific mole numbers at least until the H_2O equilibrium level is reached.

3. APPLICATION OF ONE-DIMENSIONAL MANIFOLDS TO FLAT FLAMES

In this section we describe how the reduced scheme is applied to stationary flat flames. The differential equations for the species of the full system follow from Eq. (1):

$$\dot{M} \frac{d\phi_i}{dx} - \frac{d}{dx}\left(\rho D_i \frac{d\phi_i}{dx} \right) = \rho W_i \qquad \text{for } i = 1, \ldots, n, \tag{13}$$

where $\dot{M} = \rho u$ is the constant mass flow rate. To apply the reduction method to the flat flame we have to transform the differential equations for the species to one differential equation for the controlling variable α. For the reduced scheme calculations, compositions are restricted to manifold compositions. Therefore, variations in the specific mole numbers of the different species cannot be of arbitrary magnitude; changes of the vector ϕ are restricted to movements along the manifold. To restrict the movements along the manifold, we project the differential equations of the species in the direction of the tangential direction vector of the manifold $d\boldsymbol{\phi}/d\alpha$. This gives us

$$\begin{aligned} \dot{M} \sum_{i=1}^{n} \frac{d\phi_i}{d\alpha} \frac{d\phi_i}{dx} - \sum_{i=1}^{n} \frac{d\phi_i}{d\alpha} \frac{d(\rho D_i)}{dx} \frac{d\phi_i}{dx} \\ - \sum_{i=1}^{n} \frac{d\phi_i}{d\alpha} \rho D_i \frac{d^2\phi_i}{dx^2} - \sum_{i=1}^{n} \frac{d\phi_i}{d\alpha} \rho W_i = 0. \end{aligned} \tag{14}$$

A projection method based on the eigenvectors can be used instead of Eq. 14. We have chosen to use this projection Eq. 14 because then we don't have to store the eigenvectors. This differential equation contains derivatives of ϕ_i of

all species. As the mixture compositions are always part of the manifold, we rewrite the differential equation in terms of α only, by using:

$$\phi = \phi(\alpha). \tag{15}$$

Differentiating ϕ with respect to the spatial coordinate x gives:

$$\frac{d\phi}{dx} = \frac{d\phi}{d\alpha}\frac{d\alpha}{dx} \tag{16}$$

For the second-order derivative of ϕ we find

$$\frac{d^2\phi}{dx^2} = \frac{d}{dx}\left(\frac{d\phi}{d\alpha}\frac{d\alpha}{dx}\right) = \frac{d^2\phi}{d\alpha^2}\left(\frac{d\alpha}{dx}\right)^2 + \frac{d\phi}{d\alpha}\frac{d^2\alpha}{dx^2}. \tag{17}$$

Substitution of Eqs. 16 and 17 into the differential equation for the controlling variable α, Eq. 14 finally gives

$$\dot{M}\sum_{i=1}^{n}\left(\frac{d\phi_i}{d\alpha}\right)^2\frac{d\alpha}{dx} - \sum_{i=1}^{n}\left(\frac{d\phi_i}{d\alpha}\right)^2\frac{d(\rho D_i)}{d\alpha}\left(\frac{d\alpha}{dx}\right)^2 - \sum_{i=1}^{n}\frac{d\phi_i}{d\alpha}\rho D_i\frac{d^2\phi_i}{d\alpha^2}\left(\frac{d\alpha}{dx}\right)^2 - \sum_{i=1}^{n}\left(\frac{d\phi_i}{d\alpha}\right)^2\rho D_i\frac{d^2\alpha}{dx^2} - \sum_{i=1}^{n}\frac{d\phi_i}{d\alpha}\rho W_i = 0. \tag{18}$$

This is the differential equation solved numerically for the controlling variable α for stationary flat flames. The nonlinear term $(d\alpha/dx)^2$ of the differential equation 18 is linearized by writing it as $(d\alpha/dx)_{j-1}(d\alpha/dx)_j$, where j denotes the iteration index. The remaining equation is discretized using a finite difference scheme [7]. A special gridding procedure is used to avoid interpolations on the manifold. This is done by regridding in such a way, that the values of the controlling variables in the grid points coincide with manifold (grid) points, so that no interpolation errors are made. Moreover, the regridding procedure is less expensive than the interpolation procedure: no interpolations of species and chemical source terms have to be made. The coefficients $d\phi/d\alpha$ are functions of α only, and are constant if the values of the controlling variables remain the same in the grid points. Note that this regridding procedure becomes complicated if more-dimensional geometries are used. Note that it can be used only in case of one-dimensional manifolds. For more-dimensional manifolds a similar procedure can be used to minimize the interpolation errors.

4. RESULTS

We consider the three hydrogen/air reaction systems given in Appendix A. They differ in number of species and reactions. The most simple System (I) includes species H_2, O_2, H, O, OH, and H_2O and is not physically realistic. The second System (II) also takes into account HO_2. The third System (III) additionally includes H_2O_2. It has to be stressed that it is our primary aim to test the reduction method and that the accuracy of the reaction systems itself is therefore of minor interest. For all calculations simplified transport and thermodynamic properties are used (unit Lewis numbers $Le_i = 1$, constant and for all species equal specific heat $c_{p_i} = c_p$). These approximations are not essential for the reduction method and are introduced for simplicity. In order to investigate the accuracy of the one-step reduced schemes, we compare the results with full scheme calculations, using the same approximations.

4.1 Manifold calculations

Scaled specific mole numbers $\tilde{\phi}_i$ of the one-dimensional manifold maps are given by the solid lines in Figs. 1–3 as function of the scaled H_2O specific mole numbers. The differences between System I and II are small for the species H_2 and O_2. For the radicals H, O, and OH, however, we see that the region where the radical levels are high is smaller for System II. The influence of adding HO_2 to the system is large, especially for low $\tilde{\phi}_{H_2O}$ values. Since the differences between System I and II are larger than the differences between System II and III, we focus on differences between Systems I and II mainly.

The reduction method assumes reaction groups corresponding to the largest eigenvalues in steady state. The accuracy of the reduc-

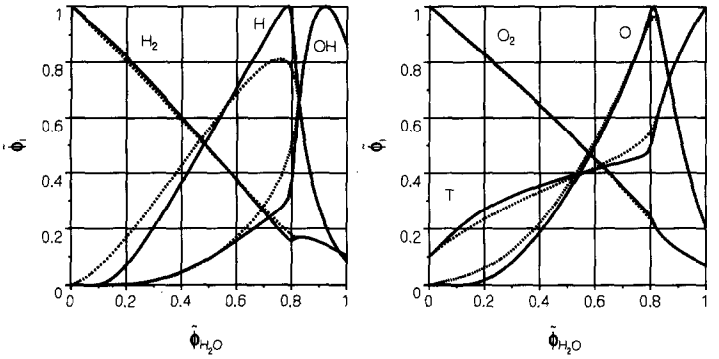

Fig. 1. Scaled specific mole numbers and temperature as function of the controlling variable $\tilde{\phi}_{H_2O}$; comparison of reduced (continuous lines) and full flat-flame calculations (dashed lines), for System I. The maximum mole fractions are: O_2, 1.5×10^{-1}; H, 9.7×10^{-2}; OH, 2.7×10^{-2}; O, 1.7×10^{-2}; H_2, 3.0×10^{-1}; H_2O, 2.7×10^{-1}, and T: 2750 K.

tion increases, if the difference between the time scales of the reaction groups that are supposed to be in steady state and the time scale of the remaining slowest process increase. Therefore, it is interesting to consider the magnitude of the real part of the eigenvalues along the manifold. Although some eigenvalues were complex during the evaluation of the manifold, they were found to be real after convergence was reached. Absolute values of the eigenvalues along the manifold are given in the Figures 4–6 for schemes I, II, and III, respectively. Since reaction system I contains six active species (and seven and eight for Systems II and III, respectively) it contains six time scales. Due to conservation of elements (O and H) two of the eigenvalues are equal to zero. The other eigenvalues are ordered in descending order of real part, i.e., eigenvalue 1 has the largest real part. Most eigenvalues are negative, only eigenvalue 1 is positive for $\tilde{\phi}_{H_2O} \lesssim 0.7$ (this is also the case for $\tilde{\phi}_{H_2O} \lesssim 0.65$ for Systems II and III). The first eigenvalue goes to zero ($\log(|\mathrm{Re}(\lambda_1)|) \to -\infty$) at the point where $\tilde{\phi}_{H_2O} \approx 0.7$ (or $\tilde{\phi}_{H_2O} \approx 0.65$). The species profiles are smooth here because the transtion of the first eigenvalue from positive values to negative values is smooth. Considering the full system (see next section) it is seen that the chemical source term of species H_2O reaches a maximum at this point ($\partial W_{H_2O}/\partial \phi_{H_2O} = 0$). Note that at $\tilde{\phi}_{H_2O} \approx 0.55$ eigenvalues 1 and 2 are not equal; eigenvalue 1 is positive and eigenvalue 2 is negative.

Comparing the specific mole numbers and eigenvalues of Systems I and II we see that, except from the fact that System II has one more eigenvalue, the specific mole numbers and the eigenvalues are not changed much for values of $\tilde{\phi}_{H_2O} \gtrsim 0.5$. One major difference is that the first eigenvalue is equal to the second one for System II near $\tilde{\phi}_{H_2O} = 0.8$ and for $\tilde{\phi}_{H_2O} \lesssim 0.22$. The reduction method is not appropriate here and the profiles of the species are therefore not smooth at $\tilde{\phi}_{H_2O} \approx 0.8$.

4.2. Flat flame calculations

Reduced and complex flat-flame calculations are performed with the three mentioned schemes. The results of the complex calculations are presented as function of $\tilde{\phi}_{H_2O}$ in Figures 1–3 by the dotted lines. The profiles of the species are also shown in Figs. 7 and 8 as

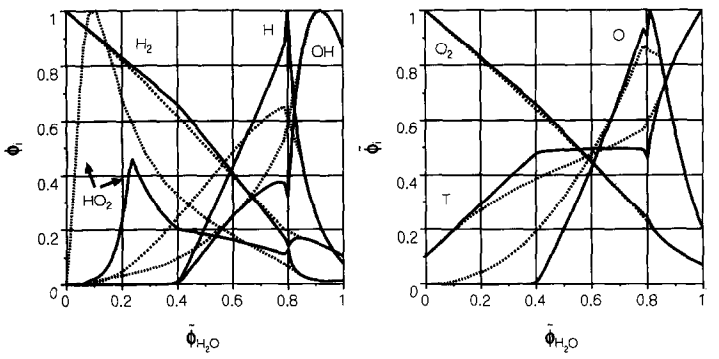

Fig. 2. Scaled specific mole numbers and temperature as function of the controlling variable $\tilde{\phi}_{H_2O}$; comparison of reduced (continuous lines) and full flat-flame calculations (dashed lines), for System II. The maximum mole fractions are: O_2, 1.5×10^{-1}; H, 8.9×10^{-2}; OH, 2.7×10^{-2}; O, 1.7×10^{-2}; H_2, 3.0×10^{-1}; H_2O, 2.7×10^{-1}; HO_2, 2.4×10^{-4}; and T, 2740 K.

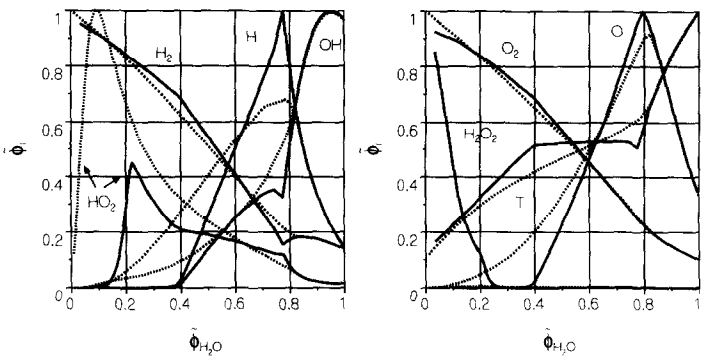

Fig. 3. Scaled specific mole numbers and temperature as function of the controlling variable $\tilde{\phi}_{H_2O}$; comparison of reduced (continuous lines) and full flat-flame calculations (dashed lines), for System III. The maximum mole fractions are O_2, 1.5×10^{-1}; H, 9.8×10^{-2}; OH, 2.7×10^{-2}; O, 1.7×10^{-2}; H_2, 2.9×10^{-1}; H_2O, 2.7×10^{-1}; HO_2, 2.4×10^{-4}; H_2O_2, 9.8×10^{-3}; and T, 2750 K. Note that the specific mole number of H_2O_2 for the full scheme is not visible in the figure because it is much smaller than for the reduced scheme.

function of x for Systems I and II. It appears that only the H-radical specific mole number is overestimated for System I. The specific mole numbers of the other species are predicted well. The differences are hardly visible in the spacial domain (Fig. 7). For System II (and III) it is seen that the difference between reduced and full scheme is large for HO_2 (and H_2O_2). Differences between other radical profiles are large around $\tilde{\phi}_{H_2O} \approx 0.8$, where the first two eigenvalues are equal. Note that overestimates of radicals are sometimes also observed in conventional reduced schemes. Comparing the mass burning rates of the complex and the reduced calculations of System I and II (Table 1), we see that the influence of adding species HO_2 to the reaction system on the mass burning rate is large. Reduced scheme calculations with schemes II (and III) predict overly low HO_2 concentrations and, therefore, underestimate the mass burning rates considerably. The influence of variations in ϕ_{HO_2} on the burning velocity is considered in more detail by considering the sensitivity of the net chemical source term $(W_{red} = (\boldsymbol{W}, \partial\boldsymbol{\phi}/\partial\alpha)/|\partial\boldsymbol{\phi}/\partial\alpha|^2)$ of the reduced scheme. The sensitivity is defined as $\partial W_{red}/\partial\phi_{HO_2}(\phi_{HO_2}/W_{red})$ and is shown in Fig. 9 for Systems II and III. It is seen that the net source term of the one-step reduced scheme strongly depends on the specific mole numbers of HO_2 for low values of $\tilde{\phi}_{H_2O}$. This explains deviations between profiles and mass burning

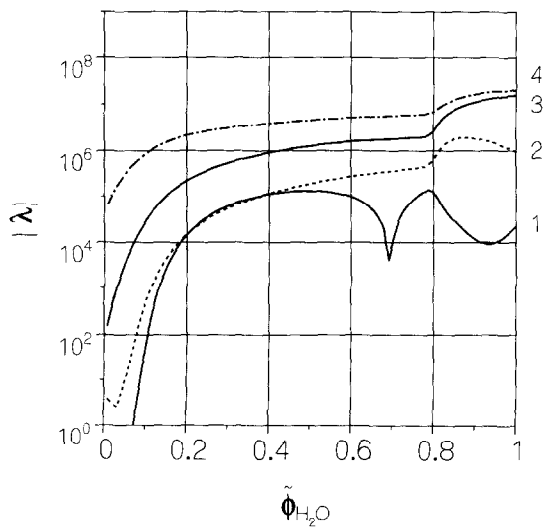

Fig. 4. Eigenvalues of the reduced hydrogen/air reaction System I.

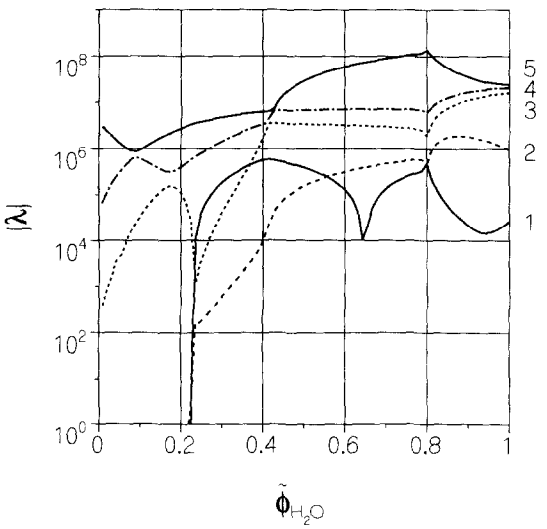

Fig. 5. Eigenvalues of the reduced hydrogen/air reaction System II. Note that eigenvalues 1 and 2 approach zero for $\tilde{\phi}_{H_2O} \lesssim 0.22$.

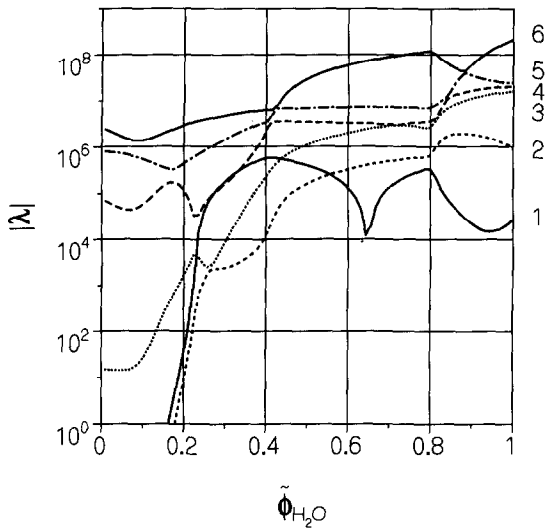

Fig. 6. Eigenvalues of the reduced hydrogen/air reaction System III. Note that eigenvalues 1 and 2 approach zero for $\tilde{\phi}_{H_2O} \lesssim 0.18$.

rates of reduced and full scheme calculations for System II and III.

5. TIME SCALE ANALYSIS OF THE FULL SYSTEM

The approximations introduced to reduce the reaction system are only appropriate if all steady-state reaction groups are faster than the remaining time scales (including convective and diffusive time scales) in the system. On the other hand, the chemical source term needs to be predicted accurately only if the time scales of the reaction system are faster than the convective and diffusive time scales.

In order to check whether this is true, we study the behavior of time scales of convection and diffusion for all species of the full reaction scheme. Therefore, we consider the conservation equation 13 of the complex system of species i. This equation contains convective ($C_i = \rho u(\partial\phi_i/\partial x)$), diffusive ($F_i = -(\partial/\partial x)\rho D_i(\partial\phi_i/\partial x)$) and chemical reaction (ρW_i) contributions. To find the typical local time scales of these terms we linearize them as follows:

$$C_i = C_i^0 + \left(\frac{\partial C_i}{\partial \phi_i}\right)^0 (\phi_i - \phi_i^0),$$

$$F_i = F_i^0 + \left(\frac{\partial F_i}{\partial \phi_i}\right)^0 (\phi_i - \phi_i^0), \tag{19}$$

$$W_i = W_i^0 + \left(\frac{\partial W_i}{\partial \phi_i}\right)^0 (\phi_i - \phi_i^0).$$

In analogy with the time scales defined by Eq. 5, the typical convective, diffusive and reaction time scales τ_i^C, τ_i^D, and τ_i^W are given by

$$\tau_i^C = \left|\rho \frac{1}{\partial C_i/\partial \phi_i}\right|,$$

$$\tau_i^D = \left|\rho \frac{1}{\partial F_i/\partial \phi_i}\right|, \tag{20}$$

$$\tau_i^W = \left|\frac{1}{\partial W_i/\partial \phi_i}\right|.$$

Note that this timescale analysis is not very accurate. However, it is useful to study the

TABLE 1

Mass Burning Rates in g/(cm^{2}s) of Adiabatic Flames Using Full and Reduced Reaction Schemes

Scheme	$\dot{M}_{complex}$	$\dot{M}_{red}$
I	0.115	0.116
II	0.195	0.155
III	0.193	0.160

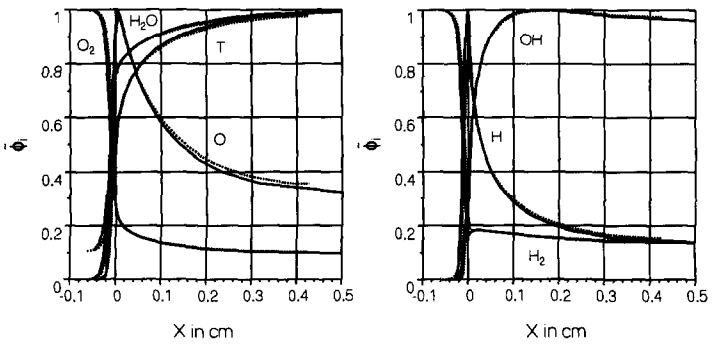

Fig. 7. Scaled specific mole numbers as functions of x; comparison of reduced (continuous lines) and full flat-flame calculations (dashed lines), for System I.

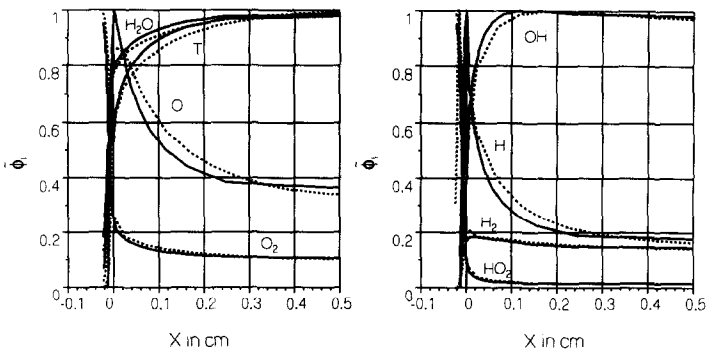

Fig. 8. Scaled specific mole numbers as function of x; comparison of reduced (continuous lines) and full flat-flame calculations (dashed lines), for System II.

contributions of the different terms in the differential equation. These time scales are calculated by using the solution of the full system. The typical time scales of H_2O are shown in Fig. 10 as function of $\tilde{\phi}_{H_2O}$ for reaction System I and II. The order of magnitude of time scales of the other species is comparable. The source term W_{H_2O} is also shown in Fig. 10. Note that the time scale of the source term $\tau^W_{H_2O}$ is infinite at the position where the source term reaches its maximum value. The time scales of convection and diffusion can also be infinite for similar reasons, e.g., the term $(\partial C^C_{H_2O}/\partial\phi_{H_2O}) = 0$ at the position where $\rho u(\partial\tilde{\phi}_{H_2O}/\partial x)$ reaches a maximum, so that $\tau^C \to \infty$ and $\log(1/\tau_{H_2O}) \to -\infty$. The time scale of diffusion is infinite when $(\partial/\partial x)$ $(\rho D_{H_2O}(\partial\phi_{H_2O}/\partial x))$ has a maximum or a minimum. These points are visible in Fig. 10 by the dips in the time-scale profiles. Considering System I in Fig. 10 we see that for $\tilde{\phi}_{H_2O} \lesssim 0.1$ convective and diffusive terms (and time scales) are of the same order of magnitude while for $\tilde{\phi}_{H_2O} \gtrsim 0.9$ convective and source terms are of the same magnitude. Note that at least two time scales must be of same order of magnitude, in order to obey Eq. 13. Also note that the behavior of the time scale of the source term in Fig. 10 resembles that of the slowest time scales of the chemical source terms of the reduced scheme (Figs. 4 and 5). This is an indication of the accuracy of the reduction technique.

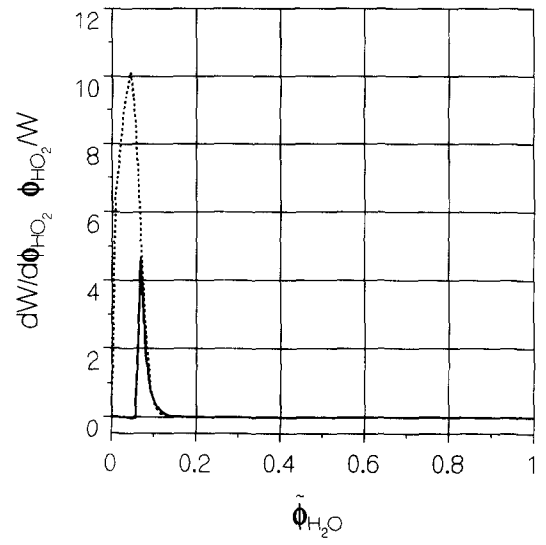

Fig. 9. Sensitivity of the net source term for the one-step reduced scheme for variations in specific mole numbers of HO_2. The continuous line denotes results for System II, the dashed line for System III.

Comparing Figs. 5 and 10 we see that the time scale of the slowest reaction group that is supposed to be in steady state is larger than convective and diffusive time scales for $\tilde{\phi}_{H_2O} \lesssim 0.22$. For $\tilde{\phi}_{H_2O} \lesssim 0.1$ the source term is small (the time scale of the source term is larger than convective and diffusive time scales), and accurate prediction of the source term is not necessary. There is, however, a region $(0.1 \lesssim \tilde{\phi}_{H_2O} \lesssim 0.22)$ where the source term may not be neglected and where the reduction method is not appropriate. This causes that the HO_2 profile, which reaches its maximum within this region, is not predicted accurately. We have already seen that variations in ϕ_{HO_2} have a large influence on the reaction rate and adiabatic mass burning rate. This brings us to the conclusion that System II (and III) cannot be reduced to an accurate one-step reduced scheme, within this region. The main reason that the one-step reduced scheme of System II and III fails is that for $\tilde{\phi}_{H_2O} \lesssim 0.22$ the second eigenvalue ap-

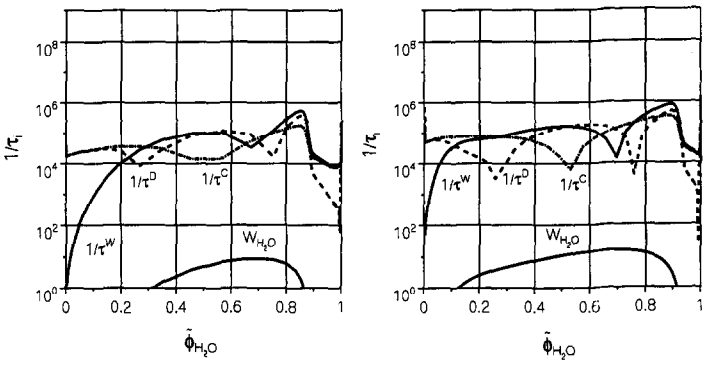

Fig. 10. Time scales of H_2O as function of $\tilde{\phi}_{H_2O}$, Systems I (a) and II (b).

proaches zero. It is likely that a two-step reduced scheme would give better results.

Now we have seen the reason of failure of one-step reduced schemes for Systems II and III, it is interesting to investigate why the one-step reduced scheme of System I gives accurate results. For this scheme the time scale of the slowest reaction group that is supposed to be in steady state is larger than convective and diffusive time scales for $\tilde{\phi}_{H_2O} \lesssim 0.2$. Here, however, the source term is already small and needn't to be predicted accurately. Although the assumptions for the reduction are not valid for this region where the source term is much smaller than convective and diffusive terms, manifold composition still may be used: radical specific mole numbers are very low at these low temperatures and as the manifold compositions satisfy the conservation equations for the elements so that $2\phi_{H_2} + \phi_{O_2} - 2\phi_{H_2O} = 0$ within this region. As we use unit Lewis numbers this is also valid for the full reaction scheme, as long as the radical specific mole numbers are small enough.

6. CONCLUSIONS

A method is presented to apply mathematically reduced reaction schemes to flat-flame calculations. It is shown that a one-step reduced scheme of the hydrogen/air reaction system gives only appropriate flat-flame results if a reaction scheme without HO_2 and H_2O_2 (System I) is used. This is caused by the fact that the steady-state assumptions are not appropriate at low temperatures where the specific mole number of species HO_2 reaches its maximum. It is found that the specific mole number of this species has a large impact on the mass burning rate. Therefore, hydrogen/air reaction systems, including species HO_2 must be reduced to more-step reduced schemes for obtaining accurate flat-flame predictions.

The support of Gastec N.V. and NOVEM, The Netherlands, is gratefully acknowledged. The authors thank U. Maas, J. ten Thye Boonkkamp and J. Nieuwenhuizen for stimulating discussions and useful suggestions.

REFERENCES

1. Maas, U., and Pope, S. B., *Combust. Flame* 88:239 (1992).
2. Peters, N., and Williams, F. A., *Combust. Flame* 68:185 (1987).
3. Peters, N., and Rogg, B., *Reduced Kinetics Mechanisms for Applications in Combustion Systems*, Springer, New York, 1993.
4. Smooke, M. D., *Lect. Notes Phys.*, 384 (1991).
5. Lam, S. H., and Goussis, D. A., *Twenty-Second Symposium (International) on Combustion*, The Combustion Institute, Pittsburgh, 1988, p. 931.
6. Goussis, D. A., and Lam, S. H., *Twenty-Fourth Symposium (International) on Combustion*, The Combustion Institute, Pittsburgh, 1992, p. 113.
7. Thiart, G. D., *Numer. Heat Transf. Part B*, 17:43 (1990).

Received 11 September 1993; revised 21 April 1994

APPENDIX: USED REACTION SCHEMES

The reaction rates of reaction i are given by the Arrhenius expression: $A_i T^{\beta_i} \exp(-E_i/RT)$, where A_i and β_i are reaction constants, E_i the activation energy, R the universal gas constant, and T the temperatures. The coefficients A_i, β_i, and E_i are successively given after the reactions (A_i in cm/mol/s; E_i in

KJ/mol). Used collision efficiencies are: $f_{H_2} = 1.00$, $f_{O_2} = 0.35$, $f_{H_2O} = 6.50$, $f_{N_2} = 0.50$, $f_{CO} = 1.50$, $f_{CO_2} = 1.50$.

A.1 System I

```
ELEMENTS
HON
END
SPECIES
O2 H OH O H2 H2O N2
END
REACTIONS KJ/MOLE
H + O2 = OH + O                          2.000E14    0.0      70.3
REV/1.46E13 0.0 2.08/
O + H2 = OH + H                          5.06E04     2.67     26.3
REV/2.24E04 2.67 18.4/
H2 + OH = H2O + H                        1.00E08     1.6      13.8
REV/4.45e08 1.6 77.13/
OH + OH = O + H2O                        1.50E09     1.14      0.42
REV/1.51E10 1.14 71.64/
H + H + M = H2 + M                       1.80E18    -1.00     0.0
H2O/6.5/H2/1.0/N2/0.5/O2/0.35/
REV/6.99E18 - 1.00 436.08/
OH + H + M = H2O + M                     2.200E22   -2.00     0.0
H2O/6.5/H2/1.0/N2/0.5/O2/035/
REV/3.80E23 - 2.00 499.41/
O + O + M = O2 + M                       2.90E17    -1.00     0.0
H2O/6.5/H2/1.0/N2/0.5/O2/0.35/
REV/6.81E18 - 1.00 496.41/
END
```

A.2 System II

Reactions and species of System I, extended with species HO_2 and the following reactions.

```
H + O2 + M = HO2 + M                     2.30E18    -0.80     0.0
H2O/6.5/H2/1.0/N2/0.5/O2/0.35/
REV/2.26E18 -0.80 195.88/
HO2 + H = OH + OH                        1.50E14     0.00     4.2
REV/1.33E13 0.00 168.3/
HO2 + H = H2 + O2                        2.50E13     0.00     2.9
REV/6.84E13 0.00 243.10/
HO2 + H = H2O + O                        3.00E13     0.00     7.2
REV/2.67E13 0.00 242.52/
HO2 + O = OH + O2                        1.80E13     0.00    -1.7
REV/2.18E13 0.00 230.61/
HO2 + OH = H2O + O2                      6.00E13     0.00     0.0
REV/7.31E14 0.00 303.53/
```

A.3 System III

Reactions and species of System II, extended with species H_2O_2 and the following reactions.

HO2 + HO2 > H202 + O2	2.50E11	0.00	−5.20
OH + OH + M = H2O2 + M	3.25E22	−2.00	0.00
REV/2.10E24 −2.00 206.80/			
H2O2 + H + H2 + HO2	1.70E12	0.00	15.70
REV/1.15E12 0.00 80.88/			
H2O2 + H = H2O + OH	1.00E13	0.00	15.00
REV/2.67E12 0.00 307.51/			
H2O2 + O = OH + HO2	2.80E13	0.00	26.80
REV/8.40E12 0.00 84.09/			
H202 + OH = H2O + HO2	5.4E12	0.00	4.2
REV/1.63E13 0.00 132.17/			